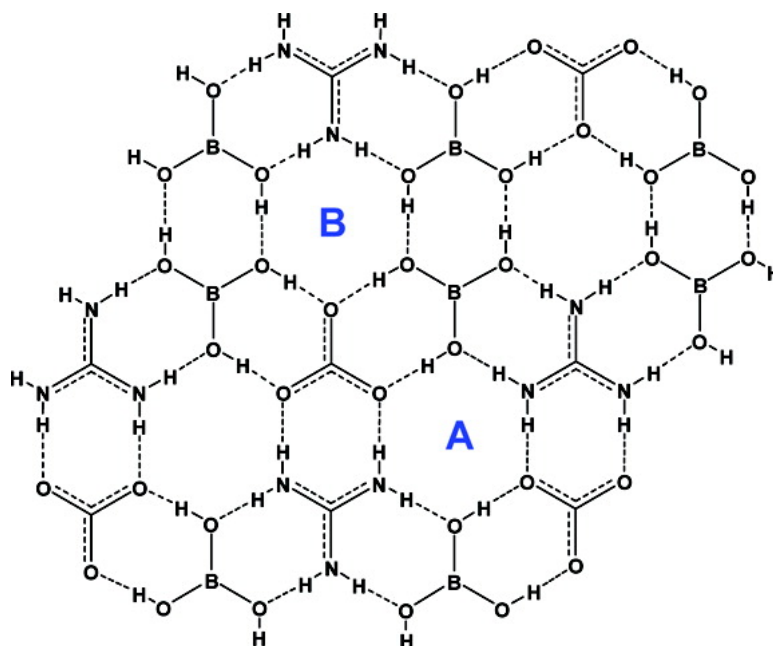


Designed Supramolecular Assembly of Hydrogen-Bonded Anionic Rosette Layers

Jie Han, Chung-Wah Yau, Chi-Keung Lam, and Thomas C. W. Mak

J. Am. Chem. Soc., **2008**, 130 (31), 10315-10326 • DOI: 10.1021/ja802425q • Publication Date (Web): 09 July 2008

Downloaded from <http://pubs.acs.org> on February 8, 2009



More About This Article

Additional resources and features associated with this article are available within the HTML version:

- Supporting Information
- Access to high resolution figures
- Links to articles and content related to this article
- Copyright permission to reproduce figures and/or text from this article

[View the Full Text HTML](#)

Designed Supramolecular Assembly of Hydrogen-Bonded Anionic Rosette Layers

Jie Han,[†] Chung-Wah Yau,[†] Chi-Keung Lam,[‡] and Thomas C. W. Mak^{*†}

Department of Chemistry and Center of Novel Functional Molecules, The Chinese University of Hong Kong, Shatin, New Territories, Hong Kong SAR, P. R. China and School of Chemistry and Chemical Engineering, Sun Yat-Sen University, Guangzhou, 510275, P. R. China

Received April 3, 2008; E-mail: tcwmak@cuhk.edu.hk

Abstract: Self-assembly of five two-dimensional hydrogen-bonded honeycomb grids bearing the rosette motif has been conducted with the guanidinium cation and various anionic components as the building blocks, tetraalkylammonium ions being employed as the interlayer templates. The sinusoidal supramolecular guanidinium–carbonate (1:1) rosette layer reported previously has been induced to adopt a nearly planar configuration using 1*H*-imidazole-4,5-dicarboxylate as an auxiliary template and spacer. A novel three-component guanidinium–boric acid–carbonate (1:2:1) wavy layer has been constructed, which features two distinguishable rosette motifs. Deviating from conventional topological design, the generation of new rosette layers, albeit highly distorted, has also been accomplished with guanidinium ions and anionic building blocks (1,2-dithiosquarate and dianionic form of 1,1'-biphenyl-2,2',6,6'-tetracarboxylate) that do not conform to C_3 -symmetry.

Introduction

Over the years, chemical entities bearing a rosette motif have attracted considerable interest in connection with supramolecular self-assembly of potentially useful organic functional materials,¹ and many studies have been conducted using computational methods² and a plethora of modern instrumental techniques.^{3–10} In the context of crystal engineering, an effective strategy of constructing a hydrogen-bonded rosette layer (often described as hexagonal honeycomb grid or sheet) is to make use of C_3 -symmetric molecular building blocks of different shapes and sizes such that their donor and acceptor sites are perfectly matched.

The sheet structure of orthoboric acid is the archetypal example of a single-component hydrogen-bonded rosette layer in which the boron atoms are arranged in a planar hexagonal array, and adjacent B(OH)₃ molecules are symmetrically linked

by a pair of O–H···O hydrogen bonds.⁴ Another single-component example is trimesic acid (1,3,5-benzenetricarboxylic acid, H₃TMA), which self-assembles through the carboxylic acid dimer motif into a honeycomb grid, whose stacking generates tunnels of net diameter ca. 14 Å for the accommodation of organic guest molecules.⁵

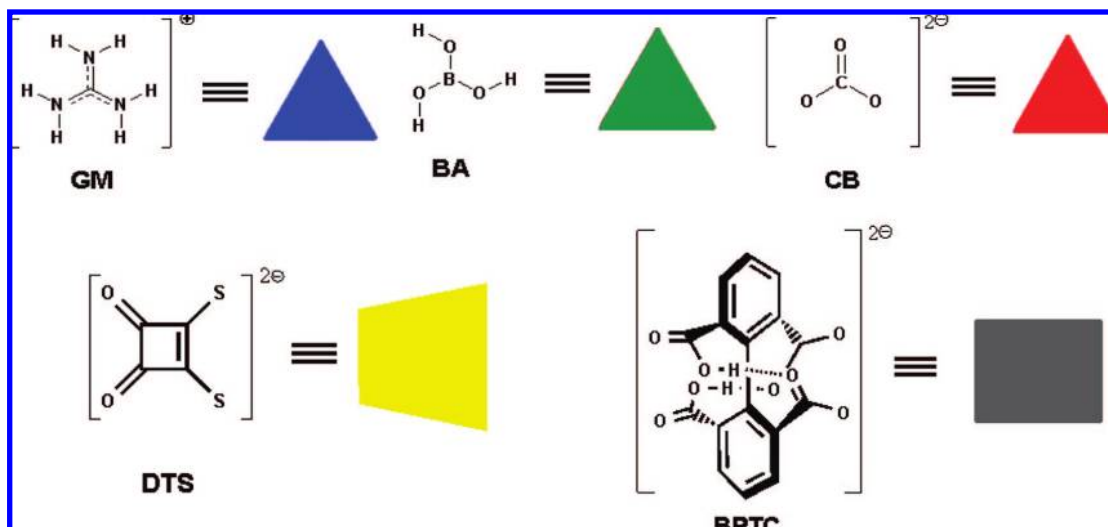
The classical example of a binary hydrogen-bonded rosette layer that was designed from first principles is the 1:1 complex of melamine with cyanuric acid,⁶ which has three hydrogen

- (3) (a) For example: Cowley, M. J.; Lynam, J. M.; Whitwood, A. C. *Dalton Trans.* **2007**, 4427. (b) Johnson, R. S.; Yamazaki, T.; Kovalenko, A.; Fenniri, H. *J. Am. Chem. Soc.* **2007**, *129*, 5735. (c) Gamez, P.; Reedijk, J. *Eur. J. Inorg. Chem.* **2006**, 29. (d) Ahn, S.; PrakashaReddy, J.; Kariuki, B. M.; Chatterjee, S.; Ranganathan, A.; Pedireddi, V. R.; Rao, C. N. R.; Harris, K. D. M. *Chem.—Eur. J.* **2005**, *11*, 2433. (e) Kerckhoffs, J. M. C. A.; van Leeuwen, F. W. R.; Spek, A. L.; Kooijman, K.; Crego-Calama, M.; Reinhoudt, D. N. *Angew. Chem., Int. Ed.* **2003**, *42*, 5717. (f) Félix, O.; Crego-Calama, M.; Luyten, I.; Timmerman, P.; Reinhoudt, D. N. *Eur. J. Org. Chem.* **2003**, 8, 1463. (g) Yagai, S.; Karatsu, T.; Kitamura, A. *Chem. Commun.* **2003**, 1844. (h) Highfill, M. L.; Chandrasekaran, A.; Lynch, D. E.; Hamilton, D. G. *Cryst. Growth Des.* **2002**, *15*. (i) Bielejewska, A. G.; Marjo, C. E.; Prins, L. J.; Timmerman, P.; de Jong, F.; Reinhoudt, D. N. *J. Am. Chem. Soc.* **2001**, *123*, 7518. (j) Mak, T. C. W.; Xue, F. *J. Am. Chem. Soc.* **2000**, *122*, 9860. (k) Jetti, R. K. R.; Thallapally, P. K.; Xue, F.; Mak, T. C. W.; Nangia, A. *Tetrahedron* **2000**, *56*, 6707. (l) Mascal, M.; Hext, N. M.; Warmuth, R.; Arnall-Culliford, J. R.; Moore, M. H.; Turkenburg, J. P. *J. Org. Chem.* **1999**, *64*, 8479. (m) Mascal, M.; Hext, N. M.; Warmuth, R.; Moore, M. H.; Turkenburg, J. P. *Angew. Chem., Int. Ed. Engl.* **1996**, *35*, 2204. (n) Simanek, E. E.; Isaacs, L.; Li, X.; Wang, C. C. C.; Whitesides, G. M. *J. Org. Chem.* **1997**, *62*, 8994. (o) Pedireddi, V. R.; Chatterjee, S.; Ranganathan, A.; Rao, C. N. R. *J. Am. Chem. Soc.* **1997**, *119*, 10867. (p) Timmerman, P.; Vreekamp, R. H.; Hulst, R.; Verboom, W.; Reinhoudt, D. N.; Rissanen, K.; Udachin, K. A.; Ripmeester, J. *Chem.—Eur. J.* **1997**, *3*, 1823. (q) Li, X.; Chin, D. N.; Whitesides, G. M. *J. Org. Chem.* **1996**, *61*, 1779. (r) Russell, K. C.; Leize, E.; Van Dorsselaer, A.; Lehn, J. M. *Angew. Chem., Int. Ed. Engl.* **1995**, *34*, 209. (s) Yang, J.; Marendaz, J.-L.; Geib, S. J.; Hamilton, A. D. *Tetrahedron Lett.* **1994**, *35*, 3665.

[†] The Chinese University of Hong Kong.

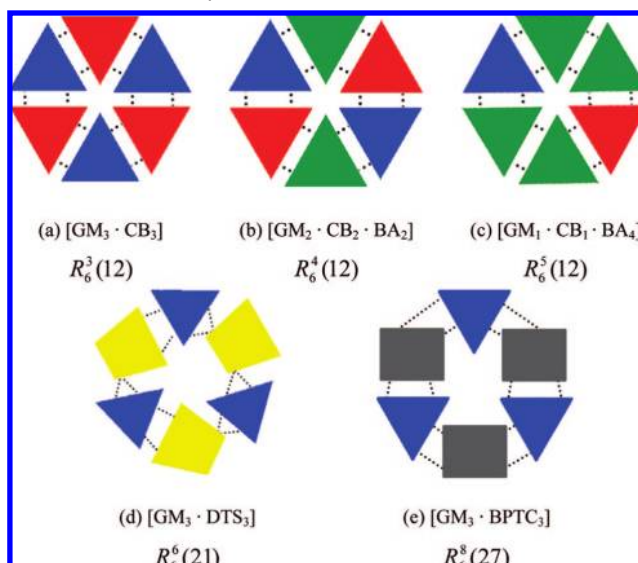
[‡] Sun Yat-Sen University.

- (1) (a) Vázquez-Campos, S.; Péter, M.; Dong, M. D.; Xu, S. L.; Xu, W.; Gersen, H.; Linderoth, T. R.; Schönherr, H.; Besenbacher, F.; Crego-Calama, M.; Reinhoudt, D. N. *Langmuir* **2007**, *23*, 10294. (b) Jonkheijm, P.; Miura, A.; Zdanowska, M.; Hoeben, F. J. M.; De Feyter, S.; Schenning, A. P. H. J.; De Schryver, F. C.; Meijer, E. W. *Angew. Chem., Int. Ed.* **2004**, *43*, 74. (c) Yagai, S.; Nakajima, T.; Karatsu, T.; Saitow, K.; Kitamura, A. *J. Am. Chem. Soc.* **2004**, *126*, 11500. (d) Kerckhoffs, J. M.; Ishi-i, T.; Paraschiv, V.; Timmerman, P.; Crego-Calama, M.; Shinkai, S.; Reinhoudt, D. N. *Org. Biomol. Chem.* **2003**, *1*, 2596. (e) Thalacker, C.; Würthner, F. *Adv. Funct. Mater.* **2002**, *12*, 209. (f) Fenniri, H.; Deng, B.-L.; Ribbe, A. E. *J. Am. Chem. Soc.* **2002**, *124*, 11064. (g) Lu, J.; Zeng, Q.-D.; Wang, C.; Zheng, Q.-Y.; Wan, L. J.; Bai, C. L. *J. Mater. Chem.* **2002**, *12*, 2856. (h) Nangia, A. *Curr. Opin. Solid State Mater. Sci.* **2001**, *5*, 115. (i) Valiyaveetil, S.; Müllen, K. *New J. Chem.* **1998**, 89.
- (2) (a) Rakotondradany, F.; Sleiman, H. F.; Whitehead, M. A. *THEOCHEM* **2007**, *806*, 39. (b) Elango, M.; Parthasarathi, R.; Subramanian, V.; Sathyamurthy, N. *J. Phys. Chem. A* **2005**, *109*, 8587.

Scheme 1. Molecular Building Blocks Employed in the Construction of Rosette Motifs and Their Graphical Representation

bonds linking every adjacent pair of its two molecular components. The same structure is also formed when cyanuric acid is replaced by thiocyanuric acid.⁷ Interestingly, recent work has demonstrated that the pet food contaminant responsible for the deaths of dogs and cats is caused by the reaction of melamine with cyanuric acid to form insoluble crystalline deposits in the animals' kidneys.¹¹

We have previously reported a hydrogen-bonded, anionic two-dimensional rosette network assembled with guanidinium and carbonate ions, which exists in the inclusion compound $4[(C_2H_5)_4N^+] \cdot 8[C(NH_2)_3^+] \cdot 3(CO_3)^{2-} \cdot 3(C_2O_4)^{2-} \cdot 2H_2O$.¹² This guanidinium–carbonate (1:1) rosette layer is folded into a pronounced plane-wave configuration via binding to other guanidinium ions, as each of its two independent carbonate ions forms 11 acceptor hydrogen bonds, only one fewer than the maximum allowable number.¹³

Scheme 2. Diagrammatic Representation of Different Rosette Motifs and Their Graph-Set Notations^a

^a (a) Two-component rosette built of C_3 -symmetric components; (b and c) three-component rosette built of C_3 -symmetric components; (d and e) rosette involving non C_3 -symmetric components.

In our ongoing design of anionic supramolecular rosette host networks using hydrophobic quaternary ammonium ions as guest templates,¹⁴ we set out to address three relevant issues. First of all, we would like to investigate whether the guanidinium–carbonate (1:1) rosette layer can be constrained to a planar configuration by the introduction of an aromatic carboxylate as a spacer. Second, we aimed at the self-assembly of the first rosette layer from three different molecular components. Finally, we tried to extend the conventional topological design of supramolecular rosette layer structures by relaxing the requirement of exact or near C_3 symmetry of the molecular building blocks. In this instance, 1,2-dithiosquaric acid and nonplanar 1,1'-biphenyl-2,2',6,6'-tetracarboxylic acid proved to be suitable starting materials for the construction of distorted hydrogen-bonded rosette layers.

- (4) Shuvalov, R. R.; Burns, P. C. *Acta Crystallogr., Sect. C* **2003**, 59, i47.
- (5) (a) Duchamp, D. J.; Marsh, R. E. *Acta Crystallogr., Sect. B* **1969**, 25, 5. (b) Herbstein, F. H.; Kapon, M.; Reisner, G. M. *J. Inclusion Phenom.* **1987**, 5, 211.
- (6) (a) Mathias, J. P.; Simanek, E. E.; Zerkowski, J. A.; Seto, C. T.; Whitesides, G. M. *J. Am. Chem. Soc.* **1994**, 116, 4316. (b) Mathias, J. P.; Seto, C. T.; Simanek, E. E.; Whitesides, G. M. *J. Am. Chem. Soc.* **1994**, 116, 1725. (c) Mathias, J. P.; Simanek, E. E.; Whitesides, G. M. *J. Am. Chem. Soc.* **1994**, 116, 4326. (d) Zerkowski, J. A.; Seto, C. T.; Whitesides, G. M. *J. Am. Chem. Soc.* **1992**, 114, 5473. (e) Seto, C. T.; Whitesides, G. M. *J. Am. Chem. Soc.* **1990**, 112, 6409. (f) Whitesides, G. M.; Simanek, E. E.; Mathias, J. P.; Seto, C. T.; Chin, D. N.; Mammen, M.; Gordon, D. M. *Acc. Chem. Res.* **1995**, 28, 37 and reference cited therein.
- (7) Ranganathan, A.; Pedireddi, V. R.; Rao, C. N. R. *J. Am. Chem. Soc.* **1999**, 121, 1752.
- (8) Katrusiak, A.; Szafranski, M. *Acta Crystallogr., Sect. C* **1994**, 50, 1161.
- (9) (a) Videnova-Adrabsinska, V.; Obara, E.; Lis, T. *New J. Chem.* **2007**, 287. (b) Russell, V. A.; Ward, M. D. *J. Mater. Chem.* **1997**, 7, 1123. (c) Russell, V. A.; Etter, M. C.; Ward, M. D. *J. Am. Chem. Soc.* **1994**, 116, 1941. (d) Holman, K. T.; Pivovar, A. M.; Swift, J. A.; Ward, M. D. *Acc. Chem. Res.* **2001**, 34, 107, and references cited therein. (e) Horner, M. A.; Holman, K. T.; Ward, M. D. *J. Am. Chem. Soc.* **2007**, 129, 14640, and references cited therein.
- (10) Melendez, R. E.; Sharma, C. V. K.; Zaworotko, M. J.; Bauer, C.; Rogers, R. D. *Angew. Chem., Int. Ed. Engl.* **1996**, 35, 2213.
- (11) Puschner, B.; Poppenga, R. H.; Lowenstine, L. J.; Filigenzi, M. S.; Pesavento, P. A. *J. Vet. Diagn. Invest.* **2007**, 19, 616.
- (12) Lam, C.-K.; Xue, F.; Zhang, J. P.; Chen, X. M.; Mak, T. C. W. *J. Am. Chem. Soc.* **2005**, 127, 11536.
- (13) Lam, C.-K.; Mak, T. C. W. *Chem. Commun.* **2003**, 2660.

- (14) Mak, T. C. W.; Li, Q. In *Advances in Molecular Structure Research*; Hargittai, M., Hargittai, I. Eds.; JAI Press: Stamford, CT, 1998; Vol. 4, pp 151–225.

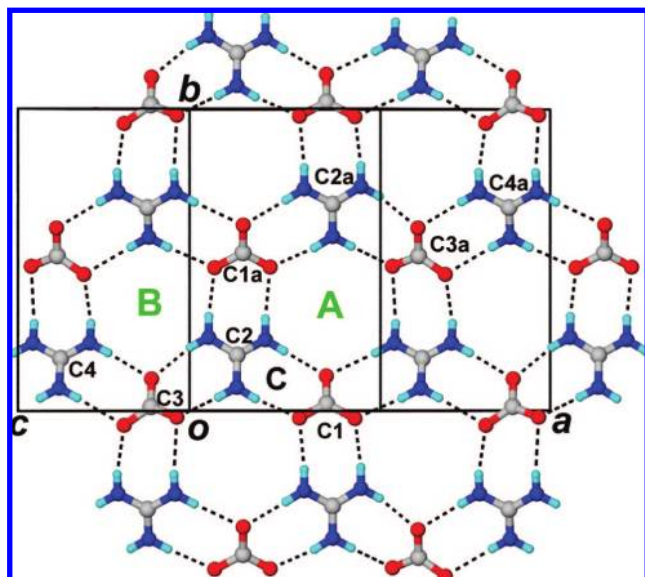


Figure 1. Projection along c^* showing the nearly planar quasi-hexagonal guanidinium-carbonate (1:1) rosette layer at $z = 1/2$ in the crystal structure of **1**. The atom types are differentiated by size and color, and N-H...O hydrogen bonds are represented by dotted lines. The layer is composed of independent carbonate ions (labeled by their central carbon atoms **C1** and **C3**) and guanidinium ions (**C2** and **C4**) in equal numbers. (Note: Mean atomic deviation from plane of one rosette = 0.36 Å, and mean atomic deviation from plane of ribbon fragment (**C1**, **C2**, **C3**, **C4**) = 0.44 Å). Symmetry transformations: a $1 - x, 1/2 + y, 1 - z$.

The squarate dianion $C_4O_4^{2-}$ has unique electronic and chemical properties in view of its idealized D_{4h} symmetry, and its charged oxygen atoms can function as strong hydrogen-bond acceptor sites.¹⁵ However, its nonbenzenoid aromatic character precludes it from masquerading as a C_3 -mimic that forms hydrogen bonds to three neighboring donors. Accordingly, we selected 1,2-dithiosquarate $C_4O_2S_2^{2-}$ in anticipation that, owing to the weakness of the (guanidinium)N-H...S hydrogen bond compared to N-H...O, the dithio analogue is better adapted to acceptor hydrogen bonding in three principal directions for the generation of a rosette network.

1,1'-Biphenyl-2,2',6,6'-tetracarboxylic acid (H_2BPTC), possessing idealized D_{2d} symmetry, is known to constitute a self-complementary hydrogen-bonding tecton with multiple donor and acceptor sites. Its dianion BPTC has a rigid nonplanar molecular skeleton held by a pair of intramolecular hydrogen bonds, so that the two phenyl rings are nearly orthogonal to each other.¹⁶ Nevertheless, although the carboxyl and carboxylate groups are widely used in forming hydrogen-bonded adducts, there are few reports of such crystal structures based on H_2BPTC and BPTC.

In the ensuing investigation, new inclusion complexes **1–5** have been obtained using various tetraalkylammonium ions as guest templates. The molecular building blocks employed in the construction of anionic host lattices are the C_3 -symmetric species guanidinium (GM), boric acid (BA), and carbonate (CB), as well as the less symmetric dianions 1,2-dithiosquarate (DTS)

- (15) (a) Lam, C.-K.; Mak, T. C. W. *Tetrahedron* **2000**, *56*, 6657. (b) Lam, C.-K.; Mak, T. C. W. *Cryst. Eng.* **2000**, *3*, 33.
 (16) Holý, P.; Závada, J.; Čisáková, I.; Podlaha, J. *Angew. Chem., Int. Ed.* **1999**, *38*, 381.
 (17) (a) Kolev, T.; Preut, H.; Bleckmann, P.; Radomirska, V. *Acta Crystallogr., Sect. C* **1997**, *53*, 805. (b) Sabareesh, V.; Ranganathan, A.; Kulkarni, G. U. Private communication, 2000.

Table 1. Structural Characteristics of Hydrogen-Bonded Rosette Networks

chemical formula	composition of rosette layer	no. of hydrogen bonds between building units	net charge of rosette layer	configuration of rosette layer	reference
H_3BO_3	boric acid	double	neutral	planar	4
$C_6H_3(COOH)_3$	trimesic acid	double	neutral	interpenetrated	5a
$C_6H_3(COOH)_3$	trimesic acid	double	neutral	pleated sheet	5b
$C_3N_3(NH_2)_3 \cdot (NH)_3(CO)_3$	melamine-cyanuric acid (1:1)	triple	neutral	nonplanar	6
$C_3N_3(NH_2)_3 \cdot (NH)_3(CS)_3$	melamine-trithiocyanuric acid (1:1)	triple	neutral	planar	7
$[C(NH_2)_3]^+ \cdot NO_3^-$	guanidinium-nitrate (1:1)	double	neutral	planar	8
$[C(NH_2)_3]^+ \cdot RSO_3^-$	guanidinium-sulfonate (1:1)	double	neutral	planar/corrugated ^a	9
$[(cyclo-C_6H_{10})_2NH_2]^+ \cdot [1,3,5-C_3H_3(COO^-)_3] \cdot xMeOH^b$	dicyclohexylammonium-trimesate (3:1) ^c	double ^d	neutral	wavy	10
$2[(C_2H_5)_4N]^+ \cdot [C(NH_2)_3]^+ \cdot [1,3,5-C_3H_3(COO^-)_3] \cdot 6H_2O$	guanidinium-trimesate (1:1)	double	anionic	planar ^e	12
$4[(C_2H_5)_4N]^+ \cdot [C(NH_2)_3]^+ \cdot 3CO_3^{2-} \cdot 3(C_2O_4)^{2-} \cdot 2H_2O$	guanidinium-carbonate (1:1)	double	anionic	wavy	12
$[C_2H_5)_4N]^+ \cdot [C(NH_2)_3]^+ \cdot 3CO_3^{2-} \cdot [C_3N_2H_2(COO^-)_2] \cdot 1$	guanidinium-carbonate (1:1)	double	anionic	nearly planar	this work
$[(n-C_3H_7)_4N]^+ \cdot [C(NH_2)_3]^+ \cdot CO_3^{2-} \cdot 2B(OH)_3 \cdot 2$	guanidinium-boric acid-carbonate (1:2:1)	double	anionic	wavy	this work
$[(n-C_4H_9)_4N]^+ \cdot [C(NH_2)_3]^+ \cdot [C_4O_2S_2^{2-}] \cdot 3$	guanidinium-dithiosquarate (1:1)	double and bifurcated	anionic	wavy	this work
$[C_2H_5)_4N]^+ \cdot [C(NH_2)_3]^+ \cdot [(C_6H_5)_2(COOH)_2(COO^-)_2] \cdot 4$	guanidinium-diphenyltetracarboxylate dianion (1:1)	double	anionic	nearly planar	this work
$[(n-C_3H_7)_4N]^+ \cdot [C(NH_2)_3]^+ \cdot [(C_6H_5)_2(COOH)_2(COO^-)_2] \cdot 5$	guanidinium-diphenyltetracarboxylate dianion (1:1)	double	anionic	pleated sheet	this work

^a The rosette layer is constructed from the cross-linkage of zigzag guanidinium-sulfonate ribbons, and the inter-ribbon dihedral angle θ_{IR} changes according to the nature of the R group, ranging from 171° for small R (methyl) to 146° for large R (2-naphthyl); a planar rosette type has $\theta_{IR} = 180^\circ$. ^b Three MeOH molecules are hydrogen-bonded to the grid outside the cavity, and there appear to be several disordered MeOH molecules within the honeycomb. ^c Adjacent trimesate ions, considered as building units, are doubly bridged by a pair of ammonium ions in an $R_2^2(8)$ motif. ^d Mediated by a pair of ammonium spacers. ^e A cyclohexane-like $(H_2O)_6$ cluster occupies the central cavity of each rosette.

Table 2. Crystallographic Data for Complex 1 to 5

complex	1	2	3	4	5
molecular formula	$[(C_2H_5)_4N^+][C(NH_2)_3^+]_7 \cdot 3CO_3^{2-} \cdot [C_3N_2H_2(COO^-)_2]$	$[(n-C_3H_7)_4N^+][C(NH_2)_3^+] \cdot CO_3^{2-} \cdot 2B(OH)_3$	$[(n-C_4H_9)_4N^+][C(NH_2)_3^+] \cdot [C_4O_2S_2^{2-}]$	$[(C_2H_5)_4N^+][C(NH_2)_3^+] \cdot [(C_6H_3)_2(COOH)_2(COO^-)_2]$	$[(n-C_3H_7)_4N^+][C(NH_2)_3^+] \cdot [(C_6H_3)_2(COOH)_2(COO^-)_2]$
molecular weight	884.98	430.12	446.71	518.56	574.67
color and habit	colorless prism	colorless block	yellow prism	colorless block	colorless block
crystal size (mm ³)	0.59 × 0.49 × 0.41	0.26 × 0.22 × 0.18	0.39 × 0.30 × 0.23	0.48 × 0.43 × 0.40	0.49 × 0.45 × 0.27
melting point (°C)	151.1–152.3	178.0–179.6	148.5–149.2	257.2–259.8	317.9–320.1
crystal system	monoclinic	orthorhombic	orthorhombic	monoclinic	monoclinic
space group	<i>P</i> 2 ₁	<i>Pnma</i>	<i>Pbca</i>	<i>P</i> 2 ₁	<i>P</i> 2 ₁ / <i>n</i>
<i>a</i> (Å)	14.406(2)	16.024(6)	16.057(2)	13.121(4)	12.239 (2)
<i>b</i> (Å)	12.042(2)	13.854(5)	16.991(2)	10.154(3)	15.769(2)
<i>c</i> (Å)	14.641(2)	11.651(4)	19.045(2)	20.248(6)	16.204(2)
α (deg)	90.00	90	90	90	90
β (deg)	117.741(4)	90	90	95.209(7)	101.315(3)
γ (deg)	90.00	90	90	90	90
<i>V</i> (Å ³)	2247.9(6)	2587(2)	5196(1)	2686(2)	3066.7(7)
<i>Z</i>	2	4	8	4	4
<i>F</i> (000)	948	936	1952	1064	1232
density (calcd) (g cm ⁻³)	1.308	1.105	1.142	1.257	1.245
θ range (deg)	1.57 to 28.27	2.28 to 28.28	2.05 to 28.31	1.01 to 26.00	1.82 to 28.35
reflections measured	15773	17137	34381	15962	21199
index ranges	$-19 \leq h \leq 16$	$-13 \leq h \leq 21$	$-21 \leq h \leq 21$	$-16 \leq h \leq 12$	$-16 \leq h \leq 16$
of measured data	$-15 \leq k \leq 16$ $-13 \leq l \leq 19$	$-18 \leq k \leq 18$ $-15 \leq l \leq 15$	$-22 \leq k \leq 22$ $-25 \leq l \leq 18$	$-12 \leq k \leq 12$ $-24 \leq l \leq 24$	$-21 \leq k \leq 20$ $-13 \leq l \leq 21$
independent reflections	10658 (0.0429)	3332 (0.0483)	6455 (0.0556)	9627(0.0364)	7634 (0.0419)
observed reflection	5103	1810	3148	5954	4415
absorption correction	multiscan	multiscan	multiscan	multiscan	multiscan
relative transmission factor	0.891	0.780	0.781	0.782	0.781
extinction coefficient	0	0	0.0020(4)	0.002 (1)	0
data (obsd)/restraints/parameters	10658/25/541	3332/14/149	6455/2/263	9627/29/725	7634/0/396
final <i>R</i> indices (obsd) ^a	<i>R</i> 1 = 0.0627 <i>wR</i> 2 = 0.1313	<i>R</i> 1 = 0.0688 <i>wR</i> 2 = 0.2183	<i>R</i> 1 = 0.0552 <i>wR</i> 2 = 0.1513	<i>R</i> 1 = 0.0668 <i>wR</i> 2 = 0.1834	<i>R</i> 1 = 0.0474 <i>wR</i> 2 = 0.1083
<i>R</i> indices (all) ^a	<i>R</i> 1 = 0.1559 <i>wR</i> 2 = 0.1646	<i>R</i> 1 = 0.1214 <i>wR</i> 2 = 0.2621	<i>R</i> 1 = 0.1273 <i>wR</i> 2 = 0.2096	<i>R</i> 1 = 0.1177 <i>wR</i> 2 = 0.2139	<i>R</i> 1 = 0.0979 <i>wR</i> 2 = 0.1373
GOF index	1.053	1.093	1.007	1.002	1.002
largest difference peak (eÅ ⁻³)	0.373, -0.330	0.534, -0.305	0.412, -0.333	0.548, -0.362	0.194, -0.197

$$^a R1 = \sum |F_o| - |F_c| / \sum |F_o|, w(F_o^2 - F_c^2)^2 / \sum w(F_o^2)^2)^{1/2}.$$

and 1,1'-biphenyl-2,2',6,6'-tetracarboxylate (BPTC), as displayed in Scheme 1. The anionic form of 1*H*-imidazole-4,5-dicarboxylic acid was also used as an auxiliary template and spacer in the synthesis of compound **1**.

The chemical formulas of inclusion compounds **1–5** and the structural characteristics of rosette layers therein, in comparison with some representative examples from the literature, are displayed in Table 1.

Table 3. Comparison of Torsion Angles^a in Related Crystal Structures Containing Squarate Ion Connected to a Guanidinium or Urea or Thiourea Species by a Pair of Hydrogen Bonds

CSD entry code	compound name	torsion angles (deg)	reference
	(tetra- <i>n</i> -butylammonium)	58.74, 52.31	this work
XAHQIG	1,2-dithiosquarate (guanidinium)		
	bis(tetraethylammonium)	-8.06, -11.75	15a
XAHQEC	squarate bis(thiourea) dihydrate		
	bis(tetraethylammonium)	-17.88, -13.20	15a
XAHQAY	squarate hexakis(thiourea)		
	bis(tetraethylammonium)	-17.54, -20.79	15a
WOWMOK	squarate tetrakis(thiourea) dihydrate		
	bis(tetra- <i>n</i> -propylammonium)	1.09, 4.18	15b
RAVWAM	squarate urea clathrate dihydrate		
QIRKAD	guanidinium hydrogen squarate	-6.23, -17.30	17a
	squaric acid urea monohydrate	13.13, 14.55	17b

^a Torsion angles C–N···O(S)–C are given for type **I** hydrogen bonds (see Scheme 3) involving the squarate ion and one guanidinium/urea/thiourea molecule.

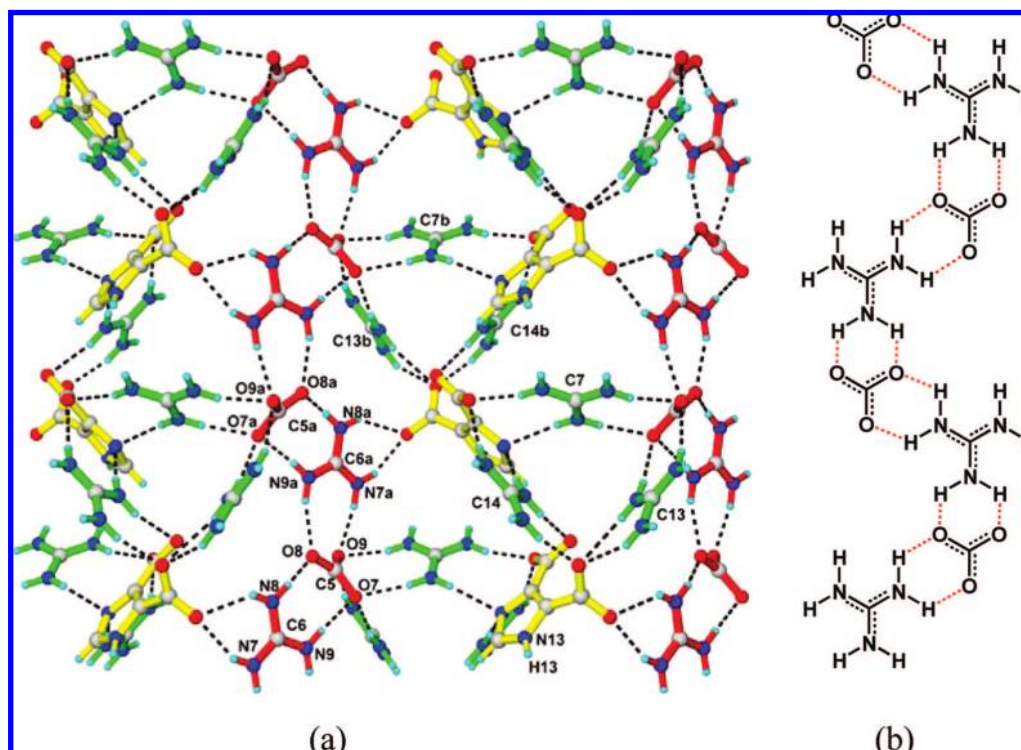


Figure 2. (a) Perspective view of the wavy layer of **1** lying in the (001) plane. The embedded crinkled tape $[\text{C}(\text{NH}_2)_3^+\text{CO}_3^{2-}]_\infty$ (colored in red) is composed of an alternate arrangement of guanidinium **C6** and carbonate **C5** ions running parallel to the *b* axis. Three guanidinium cations (**C7**, **C13**, and **C14**) constitute a “tripod” that connects to carbonate anions in the proximal rosette layer. Symmetry transformations: a $2 - x, 1/2 + y, -z$; b $1 - x, 1/2 + y, -z$. (b) Chemical structure of the crinkled tape.

Results

Complexes **1–5** are all stable crystalline materials (compound **5**, in particular, has a melting point of about 320 °C), and their crystallographic data are displayed in Table 2.

In the crystal structure of $[(\text{C}_2\text{H}_5)_4\text{N}^+] \cdot [\text{C}(\text{NH}_2)_3^+]_7 \cdot 3\text{CO}_3^{2-} \cdot [\text{C}_3\text{N}_2\text{H}_2(\text{COO}^-)_2]_2$ **1**, there are seven guanidinium and three carbonate ions in the asymmetric unit, in which two guanidinium cations (**C2**, **C4**) (designated by their central carbon atoms for convenience in description) and two carbonate anions (**C1**, **C3**) are interconnected via strong $\text{N}^+ - \text{H} \cdots \text{O}^-$ charge-

assisted hydrogen bonds to form a quasi-hexagonal supramolecular rosette layer of composition guanidinium–carbonate (1:1) exhibiting motif $[\text{A}] = R_6^3(12)$ (Figure 1). It is notable that this rosette layer has an approximately planar configuration with a mean atomic deviation of 0.44 Å, in sharp contrast to the sinusoidal wavy layer of the same composition in $4[(\text{C}_2\text{H}_5)_4\text{N}^+] \cdot 8[\text{C}(\text{NH}_2)_3^+] \cdot 3\text{CO}_3^{2-} \cdot 3(\text{C}_2\text{O}_4)^{2-} \cdot 2\text{H}_2\text{O}$.¹²

Remarkably, there is an entirely different kind of sinusoidal guanidinium–carbonate–1*H*-imidazole-4,5-dicarboxylate (4:1:1) layer (Figure 2a) that functions as a lamina between the essentially planar

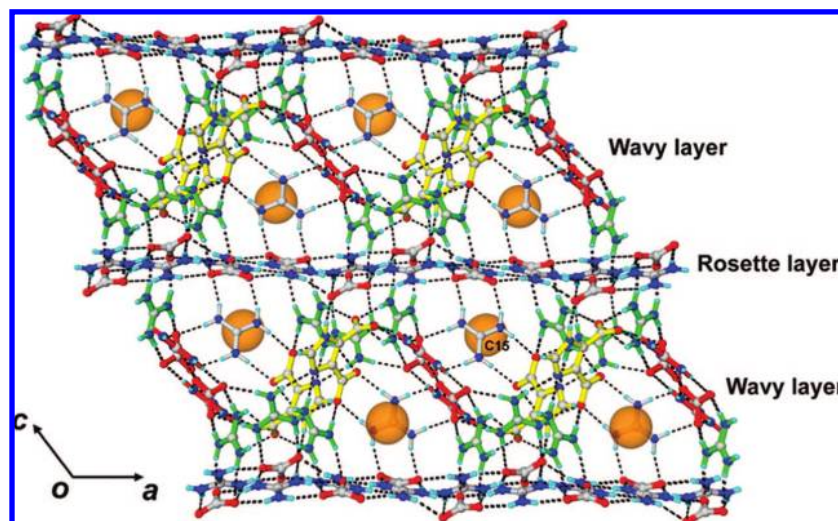


Figure 3. Projection along the *b* axis showing the crystal structure of **1**, in which the nearly planar rosette layers are sandwiched by the wavy layers. The large spheres representing the ordered Et_4N^+ cations are each accommodated inside a pocket bounded by adjacent rosette and wavy layers and closed by “windows” composed of independent guanidinium cations **C15** that stabilize the hydrogen-bonded cage work.

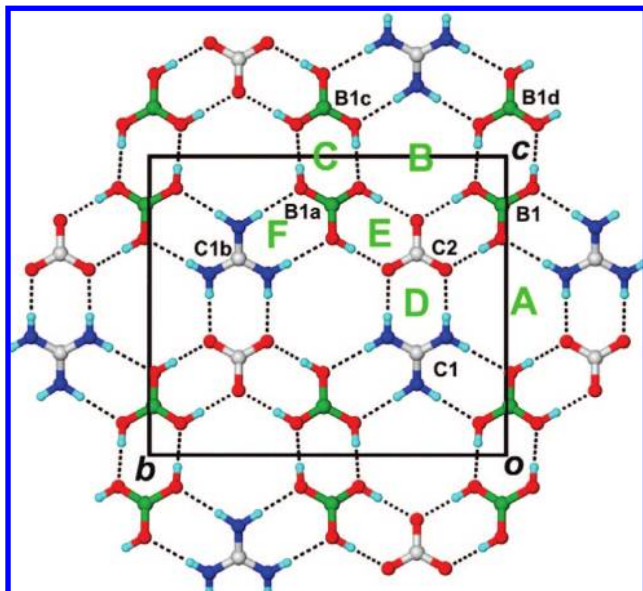


Figure 4. Projection diagram showing a portion of the guanidinium–boric acid–carbonate rosette network viewed along the a axis at $x = 1/2$ in the crystal structure of **2**. The atom types are differentiated by size and color, and $N-H\cdots O$ and $O-H\cdots O$ hydrogen bonds are represented by broken lines. The layer is composed of independent guanidinium ion **C1** (labeled by the central carbon atom), boric acid **B1**, and carbonate ion **C2** in the ratio of (1:2:1). Symmetry transformations: a $x, 0.5 - y, z$; b $1 - x, 1 - y, 1 - z$; c $1 - x, 0.5 + y, 2 - z$; d $1 - x, -y, 2 + z$. Mean atomic deviation from rosette plane: [A], 0.12 Å; [B], 0.29 Å.

guanidinium–carbonate (1:1) rosette layers. A perspective view of this wavy layer along c^* reveals that carbonate **C5** and guanidinium **C6** are joined together through pairs of $N^+-H\cdots O^-$ hydrogen bonds to create an infinite crinkled tape $[C(NH_2)_3^+CO_3^{2-}]_\infty$ that extends along the b direction (Figure 2b). Such tapes are further cross-linked through three independent guanidinium cations and one 1*H*-imidazole-4,5-dicarboxylate. As illustrated in Figure 2a, guanidinium cations **C7**, **C13**, and **C14** (depicted in green) constitute a “tripod” linker at the crest of the wavy layer, providing a total of six hydrogen-bond donor sites that bind to the carbonate anions in the rosette layer above at $N^+-H\cdots O^-$ distances ranging from 2.82 to 2.99 Å. Concomitantly, the symmetry-related “tripod” (**C7b**, **C13b**, and **C14b**) at the guanidinium cations exhibits different hydrogen-bonding environments. Guanidinium **C7** and **C13** both form a pair of $N^+-H\cdots O^-$ hydrogen bonds to the same carbonate ion from the crinkled tape; at the other side, **C7** is attached to a 1*H*-imidazole-4,5-dicarboxylate through $N^+-H\cdots O^-$ (carboxylate) and $N^+-H\cdots N$ (imidazole ring) hydrogen bonds, and **C13** is linked to a symmetry-related 1*H*-imidazole-4,5-dicarboxylate through a pair of chelating $N^+-H\cdots O^-$ (carboxylate) hydrogen bonds. Guanidinium **C14** is connected to a 1*H*-imidazole-4,5-dicarboxylate through $N^+-H\cdots O^-$ (carboxylate) and $N^+-H\cdots N$ (imidazole ring) hydrogen bonds on one side and by a pair of $N^+-H\cdots O^-$ (carboxylate) hydrogen bonds to a symmetry-related 1*H*-imidazole-4,5-dicarboxylate on the other. In addition to the “tripod” linkages above and below each wavy layer, there is an extra (imidazole)N13–H \cdots O6(carbonate **C3**) hydrogen bond with $d_{N\cdots O} = 2.84$ Å from 1*H*-imidazole-4,5-dicarboxylate in the wavy layer to carbonate **C3** which protrudes prominently out of the rosette layer.

Adjacent guanidinium–carbonate (1:1) rosette layers are thus connected by a multitude of hydrogen bonds to a sandwiched guanidinium–carbonate–1*H*-imidazole-4,5-dicarboxylate (4:1:1)

layer, which is folded and consolidated by the independent guanidinium cation **C15** (Figure 3). This guanidinium ion plays a significant role in cementing the two kinds of layers together, as it forms two pairs of strong $N^+-H\cdots O^-$ hydrogen bonds to carbonate and carboxylate groups of the wavy layer and a third pair of $N^+-H\cdots O^-$ hydrogen bonds to a carbonate group in the rosette layer, with $d_{N\cdots O}$ distances ranging from 2.84 to 3.07 Å. These quasi- C_3 symmetric interactions essentially hold neighboring layers in position in a wafer-like fashion, such that each infinite column of approximately triangular cross section, as viewed along b , is partitioned by the **C15** guanidinium ions into cavities for accommodating the hydrophobic tetraethylammonium cations.

In the crystal structure of $[(n-C_3H_7)_4N^+] \cdot [C(NH_2)_3^+] \cdot CO_3^{2-} \cdot 2B(OH)_3$ **2**, three differently charged molecular components are used to construct a hydrogen-bonded rosette layer: guanidinium **C1**, boric acid **B1**, and carbonate **C2**. The centrosymmetrically related boric acid molecules **B1a** and **B1c** are joined together through a pair of $O-H\cdots O$ hydrogen bonds of about 2.72 Å to form dimer [C] (Figure 4).

Carbonate **C2** and guanidinium **C1** both have site symmetry m and are connected pairwise through charge-assisted $N^+-H\cdots O^-$ hydrogen bonds of about 2.80 Å to form motif [D]. Notably, motifs [C] and [D] are linked together in two ways by pairs of $O_{BA}-H\cdots O_{CB}^-$ (2.56 and 2.59 Å) or $N_{GM}^+-H\cdots O_{BA}$ (2.89 and 2.93 Å) hydrogen bonds to generate motif [E] and [F], respectively. Thus three C_3 -symmetric but differently charged molecular components, namely the guanidinium cation, boric acid, and the carbonate dianion, coexist in a 1:2:1 ratio in one rosette layer with the first and last serving as hydrogen-bonding donor and acceptor, respectively. However, each boric acid molecule functions as both donor and acceptor, such that a pair of adjacent hydroxyl groups are orientated *syn-syn*, *syn-anti*, and *anti-anti*, respectively, with respect to its proximal carbonate, boric acid, and guanidinium neighbors (Figure 4). In this tertiary guanidinium–boric acid–carbonate (1:2:1) system, dimeric motifs [C], [D], [E], and [F] are interlinked to generate two distinguishable rosette motifs [A] and [B] in the same layer. Scheme 2b is a representation of the centrosymmetric $R_6^2(12)$ assembly around rosette [A], which may be designated as $[GM_2 \cdot CB_2 \cdot BA_2]$, while the $R_6^2(12)$ assembly around rosette [B] having mirror symmetry can be represented as $[GM_1 \cdot CB_1 \cdot BA_4]$, as shown in Scheme 2c.

The mean atomic deviation from the mean plane is 0.12 and 0.29 Å for rosette [A] and [B], respectively. The dihedral angle between [A] and [B] is about 24.3°, which reflects the wavy characteristics of the rosette layer.

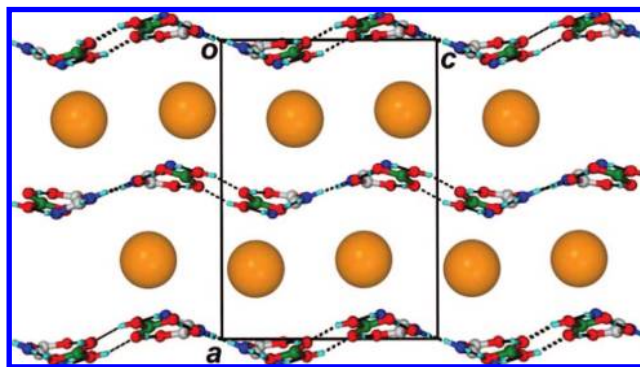


Figure 5. Packing diagram of **2** projected along the b axis, with large sphere representing the well-ordered hydrophobic $(n-Pr)_4N^+$ cations positioned regularly between adjacent wrinkled layers with an interlayer spacing of 8.01 Å.

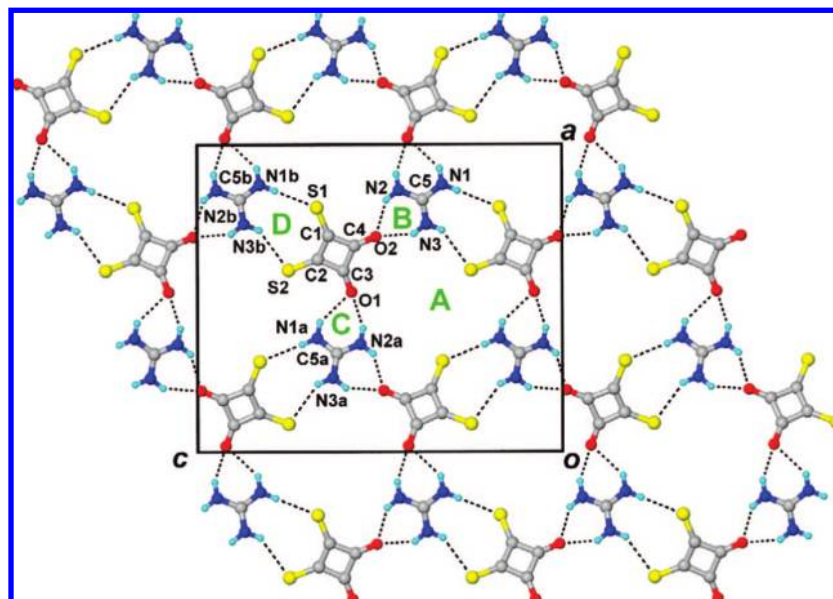


Figure 6. Projection diagram along the b axis showing a portion of the anionic rosette network at $y = 1/4$ in the crystal structure of **3**. Symmetry transformations: $a -0.5 + x, 0.5 - y, 1 - z$; $b x, 0.5 - y, 0.5 + z$. Mean atomic deviation from least-squares plane calculated from the coordinates of three GM carbon atoms plus those of one O–C–C–O fragment and two O–C–C–S fragments that constitute the interior boundary of the deformed rosette unit = 0.31 Å.

In the crystal lattice of **2**, the well-ordered tetra- n -propylammonium cation occupies a special position of symmetry m . The hydrophobic cations are located at $x \approx 1/4$ and $3/4$ and hence sandwiched between the sinusoidal rosette layers (Figure 5).

The complex $[(n\text{-C}_4\text{H}_9)_4\text{N}^+] \cdot [\text{C}(\text{NH}_2)_3^+] \cdot [\text{C}_4\text{O}_2\text{S}_2^{2-}]$ **3** has an anionic host network exhibiting a distorted quasi-hexagonal supramolecular rosette motif [A] = $R_6^0(21)$ (Figure 6). The dithiosquarate dianion carries a negative charge on each sulfur atom. It is connected to guanidinium cations C5 and C5a by chelated hydrogen bonds with the respective carbonyl oxygen atom serving as a bifurcated acceptor to form motif [B] and [C], both being $R_2^1(6)$, and also to C5b via a pair of $\text{N}^+ \cdots \text{H} \cdots \text{S}^-$ hydrogen bonds to form $R_2^2(9)$ motif [D]. The measured distances of $\text{N}^+ \cdots \text{H} \cdots \text{S}^-$ hydrogen bonds involving atoms S1 and S2 are 3.36 and 3.46 Å, respectively, and those of geminal $\text{N}^+ \cdots \text{H} \cdots \text{O}$ hydrogen bonds are 2.86 and 3.05 Å at O1, and 2.81 and 2.87 Å at O2, respectively.

Thus the guanidinium cations and dithiosquarate dianions are alternately linked to form the highly asymmetrical quasi-rosette motif [A] = $R_6^0(21)$, and the mean atomic deviation from its least-squares plane is 0.31 Å.

Figure 7a shows the stacking of slightly wavy rosette layers in the crystal structure of **3**, with an interlayer spacing of 8.45 Å ($= b/2$). Well-ordered tetra- n -butylammonium cations with the terminal methyl carbon atom of one butyl group pointing toward the central void of rosette motif [A] (Figure 7b) are sandwiched between the sinusoidal rosette layers (Figure 7a).

In the crystal structure of $[(\text{C}_2\text{H}_5)_4\text{N}^+] \cdot [\text{C}(\text{NH}_2)_3^+] \cdot [(\text{C}_6\text{H}_3)_2(\text{COOH})_2(\text{COO}^-)_2]$ **4**, the nonplanar 1,1'-biphenyl-2,2',6,6'-tetracarboxylate dianion (BPTC) replaces the planar dithiosquarate dianion as a building block to construct a supramolecular rosette layer (Figure 8). The asymmetric unit contains pairs of crystallographically independent BPTC dianions (C1, C17), guani-

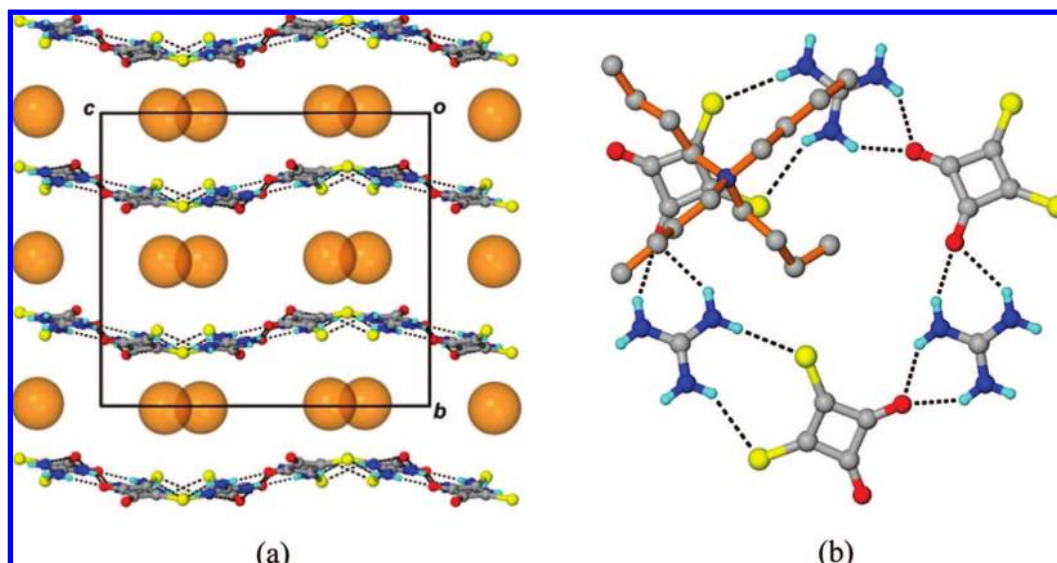


Figure 7. (a) Layer structure of **3** viewed along the a axis, with large spheres representing the ordered $(n\text{-Bu}_4)\text{N}^+$ cations that are accommodated between sinusoidal layers. (b) Terminal methyl group deviating from the main plane to point to the central void of rosette motif, as viewed along the b axis.

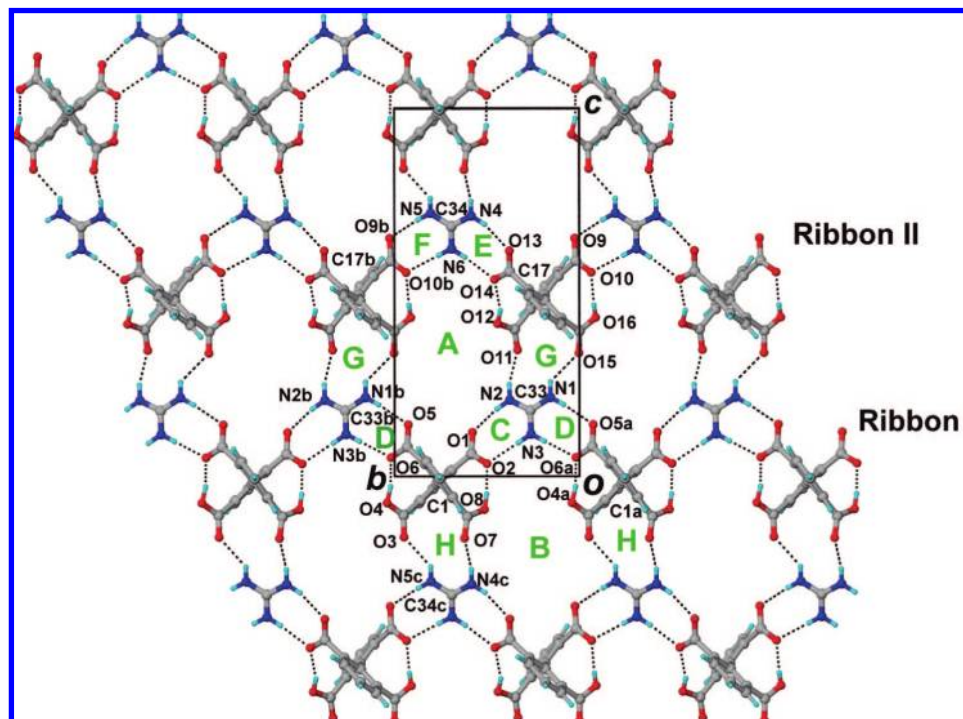


Figure 8. Projection diagram showing a portion of the anionic rosette network at $x = 1/4$ in the crystal structure of **4**. Symmetry transformations: a $x, 1 - y, z$; b $x, 1 + y, z$; c $x, y, 1 - z$.

dinium cations (**C33**, **C34**) and tetraethylammonium cations. Intramolecular linkage occurs between carboxyl and carboxylate groups attached to different phenyl rings in each tetracarboxylate dianion, forming hydrogen bonds $O4-H\cdots O6$, $O8-H\cdots O2$ in BPTC **C1** and $O16-H\cdots O10$, $O12-H\cdots O14$ in BPTC **C17**. The distances of these intramolecular hydrogen-bonds lie in the range 2.50 to 2.54 Å. In Figure 8, carboxylate oxygen atoms **O1** and **O2** come from the lower phenyl ring (view along a axis) of BPTC **C1**, and carboxylate oxygen atoms **O5** and **O6** belong to the upper phenyl ring. The pair of carboxylate groups of BPTC **C1** are linked with adjacent guanidinium cations **C33** and **C33b** by charge-assisted hydrogen bonds $N2-H\cdots O1$, $N3-H\cdots O2$, $N1b-H\cdots O5$, and $N3b-H\cdots O6$ to form $R_2^2(8)$ motif [**C**] and [**D**], yielding an infinite twisted ribbon **I** running parallel to the b axis. Similarly, motif [**E**] and [**F**] are generated by connecting guanidinium cations **C34** with BPTC **C17** and **C17b**, and further extension gives rise to ribbon **II** (Figure 8).

Ribbons of type **I** and **II** are cross-linked by pairwise $N-H\cdots O$ hydrogen bonds ranging from 2.80 to 3.02 Å between the carbonyl group of carboxylic acid and guanidinium cation via $R_2^2(13)$ motif [**G**] and [**H**] to generate similar distorted quasi-rosettes designated as [**A**] and [**B**] that exhibit the $R_3^8(27)$ motif. Rosette [**A**] is composed of two GM (**C33**), one GM (**C34**), and three BPTCs (one **C1** and two **C17**), while rosette [**B**] is composed of one **C33**, two **C34**, and three BPTCs (two **C1** and one **C17**). Figure 9 shows the packing of the approximately planar rosette layers in the crystal structure of **4**. In fact, there is no significant $\pi-\pi$ interaction between phenyl rings belonging to adjacent rosette layers. Both independent tetraethylammonium cations occupy the interlayer region; the well-ordered one is located at $x \approx 0$, and the other is disordered and located at $x \approx 1/2$.

The crystal structure of $[(n-C_3H_7)_4N^+][C(NH_2)_3^+][(C_6H_3)_2(COOH)_2(COO^-)_2]$ **5** is similar to that of complex **4**, but there is only one BPTC that possesses a pair of intramolecular

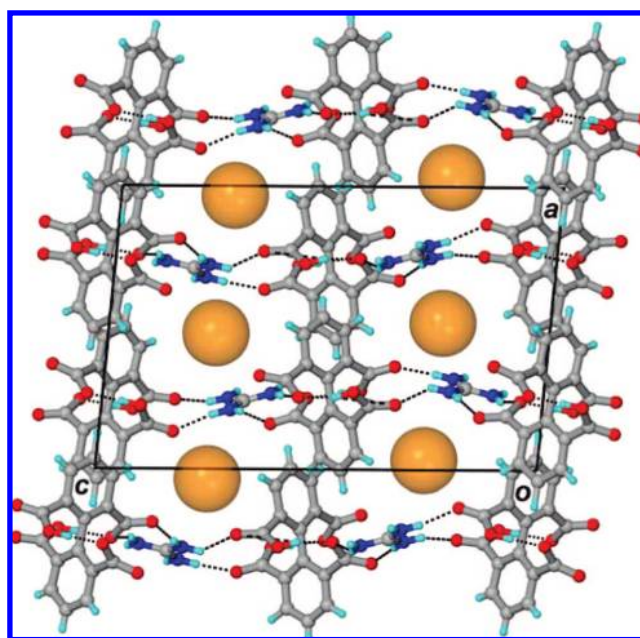


Figure 9. Approximately planar layer structure of **4** viewed along the b axis. No significant $\pi-\pi$ interaction occurs between the phenyl rings belonging to adjacent rosette layers. Both independent tetraethylammonium cations represented by the large spheres occupy the interlayer region; the well-ordered Et_4N^+ is located at $x \approx 0$, and the disordered one is located at $x \approx 1/2$.

hydrogen bonds, one guanidinium cation, and one tetra-*n*-propylammonium cation in the asymmetric unit. In complex **5**, guanidium **C17a** is linked with the upper phenyl carboxylate oxygen atoms **O1** and **O2** (viewed along the c axis) to form motif [**B**] = $R_2^2(8)$ (Figure 10). In addition, guanidinium cation **C17a** forms two donor hydrogen bonds with two carbonyl groups of adjacent BPTC **C1b** to create motif [**C**] = $R_2^2(13)$.

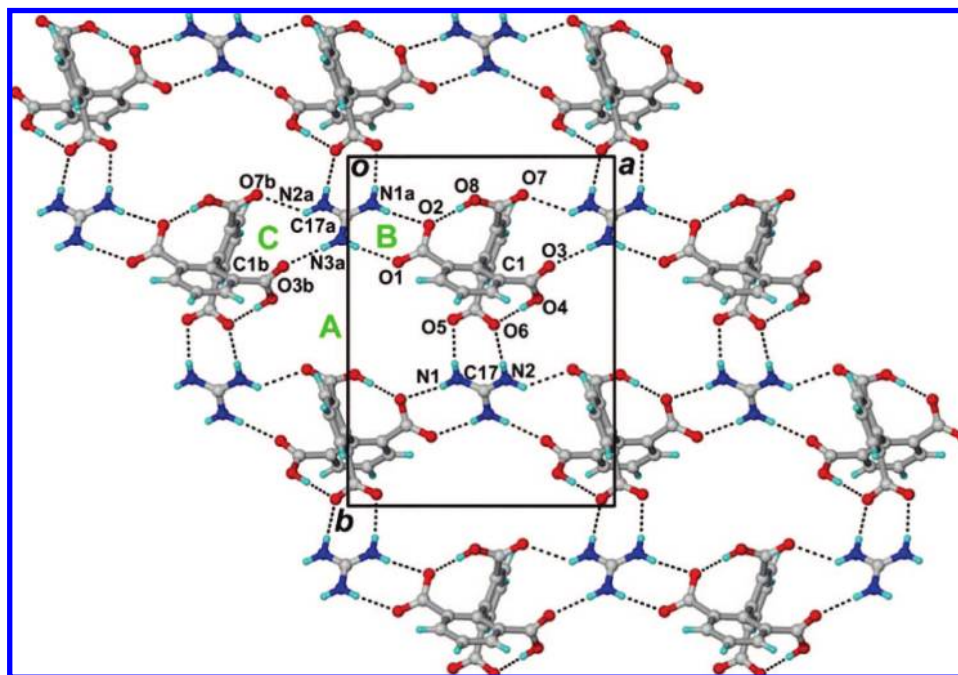


Figure 10. Projection along the c showing the quasi-hexagonal supramolecular rosette motif of **5**. Symmetry transformations: a $0.5 - x, -0.5 + y, 1.5 - z$; b $-1 + x, y, z$.

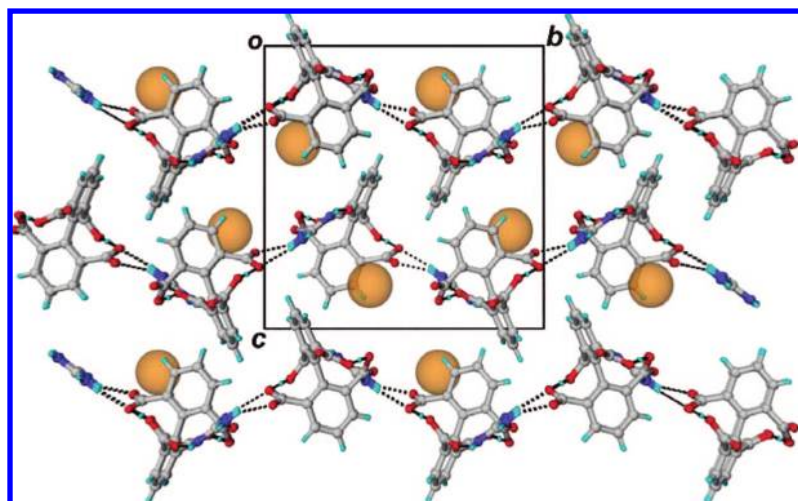


Figure 11. Crystal structure of **5**, with large spheres representing the ordered $(n\text{-Pr})_4\text{N}^+$ cations that are accommodated between the pleated sheets.

These two motifs [B] and [C] extend along the a axis to generate a parallel array of twisted ribbons. Such ribbons are consolidated by pairs of charge-assisted $\text{N1-H}\cdots\text{O5}$ and $\text{N2-H}\cdots\text{O6}$ hydrogen bonds to form the asymmetric quasi-rosette motif [A] = $R_6^8(27)$.

The distorted rosette layer of **5** takes the form of a pleated sheet, in contrast to the nearly planar configuration observed in **4**. Such sheets are concentrated at $z \approx 1/4$ and $3/4$ with the well-ordered tetra- n -propylammonium cation sandwiched in between (Figure 11).

One alkyl leg of the tetra- n -propylammonium cation extends into the central void of a rosette motif to stabilize the pleated sheet structure (Figure 12).

Discussion

In this series of five complexes, the guanidinium ion forms donor hydrogen bonds with oxygen or sulfur atoms in three

linkage modes that involve geminal hydrogen bonds (I), a pair of parallel hydrogen bonds (II), or two inclined hydrogen bonds (III) (Scheme 3).

In accordance with our initial working hypothesis, we attempted to flatten the guanidinium-carbonate (1:1) rosette layer by introducing a presumably planar aromatic carboxylate as an auxiliary template and interlayer spacer. Experimentation with a wide range of aromatic mono- and dicarboxylic acids failed to achieve our goal. Fortuitously, changing the aromatic ring to a nitrogen heterocycle made the difference, and it transpired that the use of 1*H*-imidazole-4,5-dicarboxylic acid led to the successful generation of target compound **1**, which has the composition $[(\text{C}_2\text{H}_5)_4\text{N}^+] \cdot [\text{C}(\text{NH}_2)_3^+] \cdot 3\text{CO}_3^{2-} \cdot [\text{C}_3\text{N}_2\text{H}_2(\text{COO}^-)_2]$.

In complex **1**, the guanidinium cations (C2, C4) and carbonate anions (C1, C3) that constitute the essentially planar rosette layer are interconnected via strong charge-assisted $\text{N}^+ \cdots \text{O}^-$

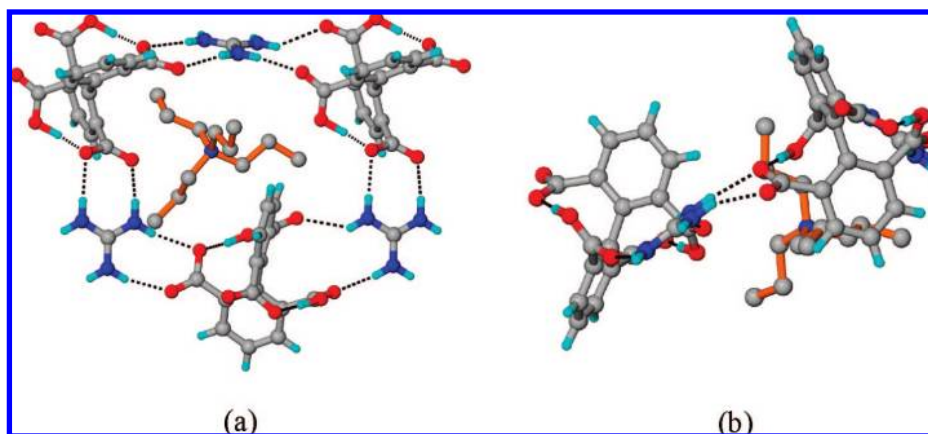
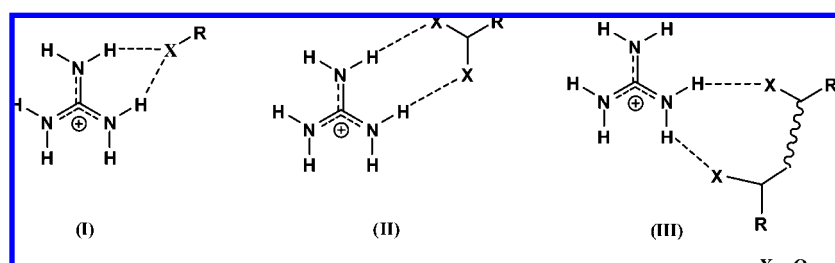


Figure 12. An alkyl leg of the tetra-*n*-propylammonium cation is inserted into the central void of the rosette motif in **5** as viewed (a) along the *c* axis and (b) along the *a* axis.

Scheme 3. Three Types of Hydrogen-Bonding Modes in Quasi-Rosette Motifs Constructed with Non- C_3 -Symmetric Dianions



hydrogen bonds with a $N\cdots O$ distance in the range 2.78 to 3.02 Å, except for a very long one at 3.37 Å involving the carbonate ion that protrudes prominently out of plane. As the carbonate ion is known to be the most prolific hydrogen-bond acceptor,¹³ additional interactions with its out-of-plane neighbors are required to satisfy its insatiable capacity. The wavy layer constructed with the 1*H*-imidazole-4,5-dicarboxylate spacer and additional guanidinium and carbonate ions serves to bind adjacent rosette layers by a multitude of hydrogen bonds in a wafer-like fashion. In contrast, in $[(n-C_3H_7)_4N^+]\cdot[C(NH_2)_3^+]\cdot CO_3^{2-}\cdot 2B(OH)_3$ **2**, the slightly wavy guanidinium–boric acid–carbonate (1:2:1) rosette layer structure stays intact without further stabilization by any interlayer linker. This is accounted for by the presence of the boric acid molecule which, by virtue of its pronounced tendency for in-plane bonding, restrains the carbonate ion from engagement in extensive out-of-plane interaction with other hydrogen-bond donor sites. The more bulky $(n-Pr)_4N^+$ cationic template may also prohibit the participation of interlayer linkers as compared with the smaller Et_4N^+ in complex **1**.

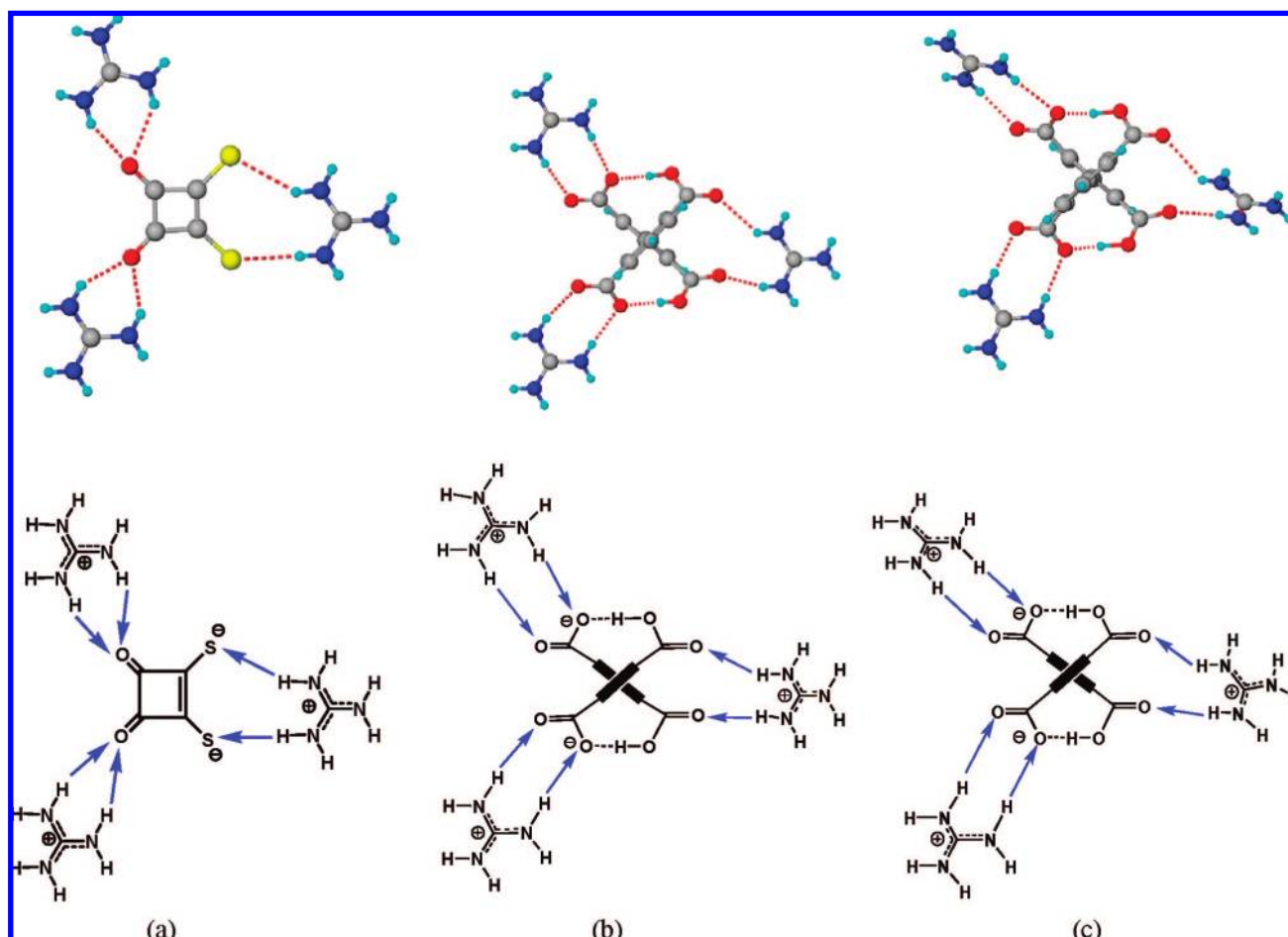
Our initial attempts to generate rosette motifs based on the squarate ion were unfruitful. However, as depicted in Figure 6, dithiosquarate is amenable to forming acceptor hydrogen bonds with GM in three directions that mimic the requirement for approximate C_3 -symmetry. As a result, its two carbonyl oxygen atoms each serve as a bifurcated acceptor in two separate directions (type **I**), whereas the sulfido terminals pair up to form a pair of acceptor hydrogen bonds along the third direction (type **II**). A comparison of the geometric parameters of $[(n-C_4H_9)_4N^+]\cdot[C(NH_2)_3^+]\cdot[C_4O_2S_2^{2-}]$ **3** with related structures composed of squarate and guanidinium/urea/thiourea shows that the C–N(guanidinium) \cdots (sulfido)S–C torsion angle of type **II** hydrogen bonds between the thiosquarate sulfur atom and GM in this case is considerably larger than that involving the squarate

oxygen atom (Table 3). This agrees with the previous finding that, in general, hydrogen bonds to sulfur not only are weaker than those to oxygen but also show a marked preference for a more “perpendicular” direction of approach to the donor atom.¹⁸

Similarly, the carbonyl group of BPTC has no strong directional preference as a hydrogen-bond acceptor, and hence it is conducive to formation of the rosette motif. The directional characteristics of the hydrogen-bonding interaction between guanidinium and BPTC in $[(C_2H_5)_4N^+]\cdot[C(NH_2)_3^+]\cdot[(C_6H_3)_2(COOH)_2(COO^-)_2]$ **4** and $[(n-C_3H_7)_4N^+]\cdot[C(NH_2)_3^+]\cdot[(C_6H_3)_2(COOH)_2(COO^-)_2]$ **5** are shown in Scheme 4. Both type **II** and **III** hydrogen-bonding modes (Scheme 3) are present, but the rosette motif in **4** is more planar than that in **5**. In complex **4**, the dihedral angle between three guanidinium cations in the same rosette motif ranges from 26° to 40°. In complex **5**, two guanidinium cations are orientated parallel to each other, whereas the third one makes a large dihedral angle of about 75° with the former two to generate a pleated sheet structure.

In comparing the rosette motifs in the present series of inclusion complexes with that in the reference compound $4[(C_2H_5)_4N^+]\cdot 8[C(NH_2)_3^+]\cdot 3(CO_3)^{2-}\cdot 3(C_2O_4)^{2-}\cdot 2H_2O$ **6**,¹² it is noted that there is considerable variation in size and shape. The shape changes from regular to irregular, and the sizes are modified significantly. For the purpose of comparison, the size of a rosette is defined by the three sides of a triangle whose vertices are the guanidinium carbon atoms. The sizes of individual rosettes in the complexes are rosette motif **A** ($7.12 \times 7.13 \times 7.38 \text{ \AA}^3$) and **B** ($6.89 \times 6.95 \times 7.03 \text{ \AA}^3$) in **1**; rosette motif **A** ($6.79 \times 6.94 \times 7.06 \text{ \AA}^3$) and **B** ($6.61 \times 6.89 \times 6.89 \text{ \AA}^3$) in **2**; ($9.26 \times 9.48 \times 9.58 \text{ \AA}^3$) in **3**; rosette motif **A** ($10.15 \times 11.09 \times 11.76 \text{ \AA}^3$) and **B** ($10.15 \times 10.97 \times 11.64 \text{ \AA}^3$) in **4**;

(18) Platts, J. A.; Howard, S. T.; Bracke, B. R. F. *J. Am. Chem. Soc.* **1996**, *118*, 2726.

Scheme 4. Three Principal Hydrogen-Bonding Directions around a Non- C_3 -Symmetric Dianion in a Distorted Rosette Layer^a

^a The surrounding guanidinium cations in complex **3** (a) and **4** (b) are almost coplanar, but one of the three guanidinium cations in complex **5** (c) is inclined to the other two by about 75°.

(10.24 × 10.24 × 10.67 Å³) in **5**; and (6.25 × 6.59 × 7.08 Å³) in **6**. The rosette units composed of non C_3 -symmetric molecular components are obviously larger than that in guanidinium–carbonate (1:1).

Conclusion

The present work has demonstrated several effective strategies toward the designed construction of hydrogen-bonded anionic rosette layers. In the case of **1**, introduction of an ancillary anion, namely 1*H*-imidazole-4,5-dicarboxylate, as an auxiliary template and interlayer spacer suffices to convert the sinusoidal guanidinium–carbonate (1:1) rosette layer to a nearly planar configuration. In complex **2**, incorporation of boric acid into the guanidinium–carbonate system generates an unprecedented tertiary rosette layer guanidinium–boric acid–carbonate (1:2:1) that features two distinct motifs.

Inherent threefold molecular symmetry used to be regarded as a sacrosanct requirement for molecular building blocks in the construction of two-dimensional hydrogen-bonded network structures bearing the rosette motif. The syntheses of complexes **3–5** showed that this condition can be relaxed to a considerable extent. Deliberate use of the dithiosquarate dianion in **3** as a substitute for a C_3 -symmetric species has proved that construction of a rosette layer is still feasible, although conspicuous deviation from perfect coupling between hydrogen-bond donor and acceptor has to be tolerated. An alternative reduction in

symmetry of the acceptor component, employing the nonplanar dianionic form of 1,1'-biphenyl-2,2',6,6'-tetracarboxylic acid, also succeeded in generating similar distorted rosette layers, as observed in **4** and **5**. The present findings nicely illustrate the general validity of isostructural exchange between equivalent building blocks in supramolecular self-assembly¹⁹ and as such provide a promising guiding principle in the crystal engineering of new rosette systems from simple molecular components.

Experimental Section

Materials and Physical Measurements. Commercially available 1*H*-Imidazole-4,5-dicarboxylic acid, guanidinium carbonate (commonly known as guanidine carbonate), aqueous tetraethylammonium hydroxide, tetra-*n*-propylammonium hydroxide and tetra-*n*-butylammonium hydroxide were used as received without further purification. Sodium dithiosquarate²⁰ and 1,1'-biphenyl-2,2',6,6'-tetracarboxylic acid²¹ were prepared according to literature methods. IR spectra were recorded with KBr pellets on a Nicolet Impact 420 FT-IR spectrometer in the region 4000–400 cm⁻¹. Melting points (uncorrected) were measured on an IA9100 Electrothermal Digital Melting Point Apparatus.

(19) (a) Kálmán, A.; Párkányi, L. In *Advances in Molecular Structure Research*; Hargittai, M., Hargittai, I. Eds.; JAI Press: Stamford, CT, 1997; Vol. 3, pp 189–226. (b) Lam, C.-K.; Mak, T. C. W. *Cryst. Eng.* **2000**, *3*, 225.

(20) Eggerding, D.; West, R. *J. Org. Chem.* **1976**, *41*, 3904.

(21) Pryor, K. E.; Shipps, G. W., Jr.; Skyler, D. A.; Rebek, J., Jr. *Tetrahedron* **1998**, *54*, 4107.

Synthesis of $[(C_2H_5)_4N^+][C(NH_2)_3^+]_7 \cdot 3CO_3^{2-} \cdot [C_3N_2H_2(COO^-)_2]$ (1). 1*H*-Imidazole-4,5-dicarboxylic acid (40 mg, 0.26 mmol) was neutralized with 2 mol equiv of aqueous tetraethylammonium hydroxide (0.52 mmol). Next, guanidinium carbonate (137 mg, 0.78 mmol) was added, and the solution was stirred for about 5 min and then filtered. The colorless filtrate was subjected to slow evaporation at room temperature in a desiccator charged with anhydrous silica gel.

Deposition of colorless rectangular prisms of **1** occurred in nearly quantitative yield over a period of several weeks. Mp 151.1–152.3 °C. IR (KBr): 3362, 3237, 3059, 2818, 2360, 1688, 1582, 1553, 1492, 1390, 1173, 1003, 949, 879, 665, 543 cm^{-1} .

Synthesis of $[(n-C_3H_7)_4N^+][C(NH_2)_3^+] \cdot CO_3^{2-} \cdot 2B(OH)_3$ (2). Guanidinium carbonate (24 mg, 0.2 mmol) and tetra-*n*-propylammonium hydroxide were mixed in a molar ratio of 1:1, and a minimum quantity of water was added to dissolve the solid. After CO_2 was bubbled through the solution for about 30 min, 2 mol equiv of boric acid aqueous solution (24 mg, 0.4 mmol) was slowly added. The solution was stirred for about 15 min and then filtered. Colorless block-like crystals of **2** were deposited in nearly quantitative yield over a period of several weeks. Mp 178.0–179.6 °C. IR (KBr): 3345, 2975, 2884, 2471, 1922, 1694, 1626, 1596, 1493, 1488, 1460, 1385, 1183, 1148, 1032, 1006, 969, 876, 836, 758, 707, 665, 570, 517 cm^{-1} .

Synthesis of $[(n-C_4H_9)_4N^+][C(NH_2)_3^+] \cdot [C_4O_2S_2^{2-}]$ (3). Aqueous tetra-*n*-butylammonium hydroxide (0.2 mmol) was added to sodium dithiosquarate (38 mg, 0.2 mmol) and guanidinium carbonate (24 mg, 0.2 mmol) and stirred for about 15 min and then filtered. The yellow filtrate was subjected to slow evaporation at room temperature in a desiccator charged with anhydrous silica gel. Deposition of **3** as yellow rectangular prisms occurred in nearly quantitative yield over a period of several weeks. Mp 148.5–149.2 °C. IR (KBr): 3362, 3135, 2959, 2937, 2874, 1705, 1646, 1631, 1555, 1483, 1336, 1324, 1201, 1151, 941, 923, 739, 630, 523 cm^{-1} .

Synthesis of $[(C_2H_5)_4N^+][C(NH_2)_3^+] \cdot [(C_6H_3)_2(COOH)_2(COO^-)_2]$ (4). 1,1'-Biphenyl-2,2',6,6'-tetracarboxylic acid (33 mg, 0.1 mmol) was neutralized with 2 mol equiv of aqueous tetraethylammonium hydroxide (0.2 mmol). Next, guanidinium carbonate (12 mg, 0.1 mmol) was added, and the solution was stirred for about 15 min and then filtered. The colorless filtrate was subjected to slow evaporation at room temperature in a desiccator charged with anhydrous silica gel. Deposition of **4** in the form of colorless blocks occurred in nearly quantitative yield over a period of several weeks. Mp 257.2–259.8 °C. IR (KBr): 3430, 2993, 2610, 1730, 1715,

1698, 1613, 1579, 1463, 1435, 1388, 1236, 1176, 1150, 1034, 1000, 883, 821, 779, 697, 669, 654, 577 cm^{-1} .

Synthesis of $[(n-C_3H_7)_4N^+][C(NH_2)_3^+] \cdot [(C_6H_3)_2(COOH)_2(COO^-)_2]$ (5). 1,1'-Biphenyl-2,2',6,6'-tetracarboxylic acid (33 mg, 0.1 mmol) was neutralized with 2 mol equiv of aqueous tetra-*n*-propylammonium hydroxide (0.2 mmol). Next, guanidinium carbonate (12 mg, 0.1 mmol) was added, and the solution was stirred for about 15 min and then filtered. The colorless filtrate was subjected to slow evaporation at room temperature in a desiccator charged with anhydrous silica gel. Compound **5** was obtained as colorless block-like crystals in nearly quantitative yield over a period of several weeks. Mp 317.9–320.1 °C. IR (KBr): 3359, 3168, 2975, 2885, 1688, 1607, 1557, 1473, 1435, 1385, 1336, 1270, 1141, 988, 837, 820, 790, 764, 693, 625, 578, 556, 526 cm^{-1} .

X-ray Crystallography. Intensity data of compound **1** to **5** were collected on a Bruker SMART 1000 CCD system with Mo $K\alpha$ radiation ($\lambda = 0.71073 \text{ \AA}$) from a sealed-tube generator at 293 K. Data collection and reduction were performed using SMART and SAINT software,²² and empirical absorption corrections were applied.²³ All the structures were solved by direct methods and refined by full-matrix least-squares on F^2 using the SHELXTL program package.²⁴

Acknowledgment. This work is dedicated to the memory of Prof. George Alan Jeffrey (1915–2000). This work is funded by the Hong Kong Research Grants Council (CERG ref No. CUHK 402003 and 402406) and the Wei Lun Foundation. C.-K.L. acknowledges financial support by the Natural Science Foundation of China (No. 20503041).

Supporting Information Available: X-ray crystallographic data for inclusion compounds **1–5** in CIF format. This material is available free of charge via the Internet at <http://pubs.acs.org>.

JA802425Q

- (22) Bruker SMART 5.0 and SAINT 4.0 for Windows NT: Area Detector Control and Intergration Software; Bruker Analytical X-Ray Systems, Inc.: Madison, Wisconsin, USA, 1998.
- (23) Sheldrick, G. M. SADABS: Program for Empirical Absorption Correction of Area Detector Data; University of Göttingen: Göttingen, Germany, 1996.
- (24) Sheldrick, G. M. SHELXTL 5.10 for Windows NT: Structure Determination Software Programs; Bruker Analytical X-Ray Systems, Inc.: Madison, Wisconsin, USA, 1998.